Journal of Magnetism and Magnetic Materials 563 (2022) 169975

Contents lists available at ScienceDirect

Journal of Magnetism and Magnetic Materials

journal homepage: www.elsevier.com/locate/jmmm

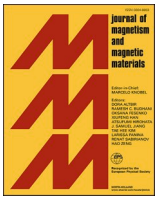

Fe_xCo_{1-x} alloy nanoparticles: Synthesis, structure, magnetic characterization and magnetorheological application

Virginia Vadillo [a], Maite Insausti [a,b], Jon Gutiérrez [a,b,*]

[a] BCMaterials, Basque Center for Materials, Applications and Nanostructures, UPV/EHU Science Park, Bldg. Martina Casiano, Barrio Sarriena, s/n, 48940 Leioa, Spain
[b] Faculty of Science and Technology, University of the Basque Country UPV/EHU, Barrio Sarriena s/n, 48940 Leioa, Spain

ARTICLE INFO

Keywords:
FeCo alloy
Magnetic nanoparticles
Magnetorheological application

ABSTRACT

We present results concerning the synthesis of Fe_xCo_{1-x} ($0 < x < 1$) alloy nanoparticles (NPs) with different compositions by the chemical reduction technique and subsequent structural (XRD patterns), morphological (TEM images) and magnetic (VSM magnetometry) characterization. We have got excellent quality NPs in the cubic bcc structure showing a room temperature magnetization as high as 235 emu/g for the $Fe_{66}Co_{34}$ composition alloy. Powder of composition $Fe_{47}Co_{53}$ was used to fabricate a magnetorheological fluid (MRF) by using mineral oil as carrier liquid and Aerosil 300 as additive to control the viscosity of the fluid. This MRF showed a strong magnetorheological response with a superior performance under applied magnetic field up to 616.7 kA/m and good reversibility after demagnetization process. At that highest applied magnetic field, we determined a yield stress value of 2729 Pa, that competes well with the best ones reported in the most recent literature.

1. Introduction

The FeCo alloy is a soft ferromagnetic material of great interest not only from the point of view of fundamental structural and magnetic properties but also for technological applications. This alloy shows the highest known magnetization (above 230 emu/g), large permeability, low coercivity, and high Curie temperature (about 1000 K) [1,2]. These excellent soft magnetic properties are responsible for this alloy to be of special interest for applications, being at the moment the actual trend its fabrication at the "*nano*" scale. The FeCo particles applications extend from magnetic recording media [3] or exchange-coupled nanocomposite magnets [4] to heat generation mechanisms by submitting them to an external AC excitation magnetic field [5]. One of the most recent applications involves the use of FeCo soft magnetic nanoparticles (NPs) embedded in a polymeric or fluidic matrix, in order to develop magnetic stimuli-responsive materials or the so called "smart polymers and fluids" (see for example [6] and references therein).

Through the literature, FeCo alloy nanoparticles have been extensively synthesized by following either chemical (such us thermal [7,8] or reductive [9,10] decomposition of metallic precursors, polyol-assisted processes [11,12] or some attemps with microwave assisted methods [13]) or physical routes (like surfactant-assisted ball milling [5,14] or laser ablation technique [15,16]). Most of these fabrication methods have been mainly focused on one or two nearly equiatomic Fe_xCo_y ($x \approx y$) alloy compositions, and in general good structural and magnetic properties are achieved. Nevertheless, different synthesis processes are sometimes followed by a wide variety of results in the obtained particle morphology, as nanoflakes-like [14], needle-like [17], or even too small [5] synthesized nanoparticles. It is also not unusual the appearance of impurities like magnetite (Fe_3O_4) [18]. In all these mentioned cases (see, for example, [5,12,17,18]) the direct consequence is a lower value of the measured magnetization than the expected one (usually above 200 Am^2/kg).

Moreover, few works have investigated the synthesis and the measured properties of the family of alloys Fe_xCo_{1-x} (see, for example, [19–22]). Bearing all these previous considerations in mind, in this work we present an exhaustive study of the Fe_xCo_{1-x} family of nanoparticles (NPs) synthesized by employing the chemical reduction route and with different compositions: pure Fe ($x = 1$), Fe_xCo_{1-x}: Fe excess ($x/(1-x) > 1$), FeCo: equiatomic ($x/(1-x) = 1$ or $x = 1/2$), Fe_xCo_{1-x}: Co excess ($x/(1-x) < 1$) and pure Co ($x = 0$). Three of the synthesized compositions belong to the FeCo binary alloy. We have performed the structural, morphological and magnetic characterization of the synthesized five different nanoparticles compositions, telling us immediately about the good

* Corresponding author at: Faculty of Science and Technology, University of the Basque Country UPV/EHU, Barrio Sarriena s/n, 48940 Leioa, Spain.
E-mail address: jon.gutierrez@ehu.eus (J. Gutiérrez).

https://doi.org/10.1016/j.jmmm.2022.169975
Received 9 May 2022; Received in revised form 18 July 2022; Accepted 15 September 2022
Available online 24 September 2022

quality and excellent magnetic characteristics of the obtained product. Finally, we will show the behavior of a magnetorheological fluid (MRF) fabricated with nanoparticles of composition $Fe_{47}Co_{53}$ prepared by following the same previously used chemical reduction route. This alloy also shows good soft magnetic properties that will be reflected in a MRF with a superior performance as it will be shown in the following.

2. Materials and methods

Iron-cobalt Fe_xCo_{1-x} ($0 < x < 1$) nanoparticles (NPs) with different compositions were synthesized by employing a chemical reduction technique. In this method, aluminium powder was employed as agent to reduce Fe (III) and Co (II) precursors in the presence of NH_4F. Extensive information about the preparation method for the equiatomic composition can be found in a previous work of the authors [6].

The structure of the synthesized Fe_xCo_{1-x} nanoparticles was determined by X-ray diffraction measurements. XRD data were collected by using a Bruker D8 Advance diffractometer equipped with a copper anode ($\lambda = 1{,}5406$ Å, operated at 40 kV and 40 mA), Ge(1 1 1) incident beam monochromator and 1-D LynxEye detector (active length in 2θ 2,7°). The sample was mounted on a zero-background silicon wafer embedded in a generic sample holder. Data were collected in the $2\theta = 30°–155°$ range (step size 0.03 and time per step = 20 s) at RT. A fixed divergence and antiscattering slit 1° giving a constant volume of sample illumination were used. Their morphology as raw powder was analyzed by Transmission Electron Microscopy (TEM) technique. TEM images were obtained using a Philips CM200 microscope at an acceleration voltage of 200 kV. For samples preparation, Fe, Co and FeCo alloy nanoparticles with different compositions were first dispersed in hexane and drop-casted onto a copper grid. To estimate the nanoparticles (or their agglomerates) size, ImageJ software was used [23].

In order to determine the final Fe to Co content ratio and so the final composition of the obtained product after each synthesis, Inductively Coupled Plasma-Mass (ICP) Spectrometry technique was used by employing an ICP-MS (7700x, Agilent Technologies) spectrophotometer. For this measurement, 30 mg of each Fe_xCo_{1-x} nanoparticle composition were previously dissolved in 2 ml of an acid solution (nitric acid- hydrochloric acid ratio 1:1).

Magnetic properties were determined through measured M(H) hysteresis loops at room (298 K) temperature, by using a vibrating sample magnetometer (VSM).

3. Results and discussion

3.1. Structural and morphological characterization

The final product of each chemical reduction process is a black powder that was collected magnetically, it was washed with distilled water and ethanol and dried at room temperature. The achieved amount of sample varies in the 0.8–1 g range per process. The following step was to check the final composition of the obtained powders, as well as their structure. Thus, Table 1 summarizes the different Fe_xCo_{1-x} NPs compositions synthesized and the molar ratio of the employed precursors during the chemical reduction method, as well as the expected and obtained final compositions.

In all the synthesized alloy samples, the final Fe/Co ratio is lower than the initially expected one from the 1.25:0.5, 1:0.75 and 0.7:1.05 mol-ratio of the Fe and Co precursors used for the synthesis, respectively. Besides, a small amount of aluminium appears as impurity (in the range 0.3–0.5 %at), most probably due to the excess of aluminium used in the synthesis in order to improve the reaction yield.

Fig. 1 shows the obtained XRD patterns for the different Fe, Co and FexCo1-x alloy synthesized nanoparticles. Structural data were refined by Rietveld procedure and the fitted diffraction patterns are displayed in the Supporting Information (Fig. S1, Table S1), being included in Table 1 the calculated lattice parameters. The pure Fe powder diffraction

Table 1
Ratio of employed precursors for the different Fe, FexCo1-x alloys and Co NPs synthesized by chemical reduction method, as well as the expected and obtained final compositions. Determined cell parameters and average grain sizes from XRD measurements are also shown.

Sample	Fe (III): Co(II) mol-ratio	Expected sample composition	ICP composition	Lattice parameter *a* (Å)	Average grain size (nm)
Fe	1,75: 0	Fe	Fe	2,8659(1)	46(4)
FeCo (Fe excess)	1,25: 0,5	$Fe_{71}Co_{29}$	$Fe_{66}Co_{34}$	2,8626(1)	44(4)
FeCo (1:1)	1: 0,75	$Fe_{57}Co_{43}$	$Fe_{51}Co_{49}$	2,8562(1)	28(2)
FeCo (Co excess)	0,7: 1,05	$Fe_{40}Co_{60}$	$Fe_{33}Co_{67}$	2,8405(2)	31(2)
Co	0: 1,75	Co	Co	2,5056(2) *c* = 4,0681 (5)	28(2)

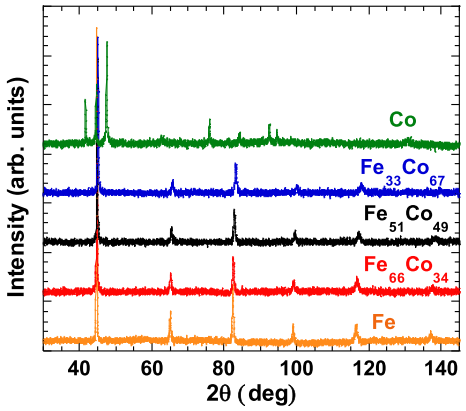

Fig. 1. Room temperature XRD patterns for the different Fe, Fe_xCo_{1-x} and Co NPs synthesized by the chemical reduction method.

pattern shows the typical peaks ((1 1 0) at 44.68°, (2 0 0) at 65.02°, (2 1 1) at 82.34°, (2 2 0) at 98.95°, (3 1 0) at 116.39° and (2 2 2) at 137.18°) of the α-bcc structure with Im-3 m space group and cell parameter $a = 2.8659(1)$ Å.

The Co diffractogram pattern shows the typical peaks ((1 0 0) at 41.58°, (0 0 2) at 44.50°, (1 0 1) at 47.46°, (1 1 0) at 75.88°, (1 0 3) at 84.10° and (1 1 2) at 92.46°) of the hcp structure with P 6_3/mmc space group and cell parameter $a = 2.5056(2)$ Å and $c = 4.0681(5)$ Å. The worse fitting of experimental intensities to theoretical ones (see Fig. S1) can be ascribed to preferred orientations of some crystal faces in these nanoparticles.

Nevertheless, the peaks and intensities of the diffraction patterns of the Fe_xCo_{1-x} alloys match well with bcc-Fe, without traces of secondary phases. All maxima are slightly shifted towards 2θ lower angles, that is higher d-spacing, with increasing Fe composition. This is in good concordance with the larger atomic radius of iron ($r_{atom\text{-}Fe} = 156$ pm) comparing with cobalt ($r_{atom\text{-}Co} = 152$ pm). This effect would induce a progressive expansion of the unit cell and volume with increasing the iron content in the nanoparticles.

The crystalline grain size was calculated by using the Scherrer's formula $\tau = K\lambda/(\beta\cos\theta)$, where τ is the average size of the crystalline domains, K is the dimensionless shape factor which depends on the shape of the particles, λ is the X-ray wavelength, β is the full width at half maximum (FWHM) and θ is the corresponding Bragg angle (see Table S2). The estimated crystallite sizes are in the range among 28–46

nm and appear summarized in Table 1.

The morphology of the fabricated raw powder of the Fe_xCo_{1-x} nanoparticles has been studied by analysing TEM images. As a general trend, the smallest nanoparticles present irregular shape and non-homogeneous sizes, ranging between 20 and 60 nm, values very close to those obtained from X ray diffraction.

It has been observed that in all cases there is a strong tendency to aggregation due to their strong magnetic character (high magnetization value, as it will be seen in the following section). The size of these aggregates can reach values of 200–500 nm and, in some cases, they show a dendritic configuration (see Fig. 2). Similar aggregates have also been observed in other alloys in spite of the synthesis method employed. As an example, microwave synthesis was used for the preparation of FePt alloy nanoparticles with more homogeneous sizes (20–30 nm) although agglomerates over 200 nm also appeared [24].

3.2. Magnetic characterization

Room temperature measured hysteresis loops are shown in Fig. 3a. For all our fabricated Fe, Co and Fe_xCo_{1-x} nanoparticles, we have observed rapid saturation with low hysteresis (see Table 3), confirming so the soft magnetic character of all fabricated different composition nanoparticles.

The addition of cobalt, up to 30 %wt. (see Fig. 3b), increases the magnetization of the FeCo alloy, composition at which the alloy has the highest M_S value at room temperature than any other known material. As it can be observed, the measurements in all synthesized NPs present values of room temperature saturation magnetization slightly lower than the expected one. This is an usual observation for magnetic materials at the nanoscale as the authors have already observed [26], and it is usually ascribed to the potential spin disorder arisen due to surface effects.

Searching for information about the magnetic anisotropy of our FeCo alloys, we have used the well-known *law of approach to saturation* (LAS) that tells us that near saturation M_S the value of magnetization can be sufficiently expressed as [27,28]:

$$M \cong M_S\left(1-\frac{b}{H^2}\right)$$

where in the case of cubic symmetry $b = \frac{8}{105}\left(\frac{K_{eff}}{\mu_0 M_S}\right)^2$ [29]. So, we have performed this type of fit in our alloys in the range 0.5–3 Tesla (high field values). A typical obtained fitting curve for the alloy of composition $Fe_{51}Co_{49}$ can be shown in Fig. 4.

From the b best value obtained for the fit, we can estimate a value of the effective anisotropy K_{eff} in the alloy. Thus, for the $Fe_{51}Co_{49}$ composition, we have obtained values of $b = 6 \times 10^{10}$ $(A/m)^2$, being the subsequently estimated $K_{eff} \approx 2$ MJ/m^3. Results for the other two alloys are similar. The expected value of magnetic anisotropy for $Fe_{50}Co_{50}$ bulk alloy is about 15–20 kJ/m^3 [30]. Nevertheless, higher determined values of the anisotropy for similar compositions are also found in literature, for example Zehani *et al.* found values of 92 kJ/ m^3 for $Fe_{55}Co_{45}$ [31] and Ibrahim *et al.* reported 0,38 MJ/m^3 for $Fe_{50}Co_{50}$ [32], both at the nanoscale. The origin of such high values must be regarded mainly, among others, as a) due to strong shape effects of the single nanoparticles [33] or b) arising from distortions of the initially determined α-bcc cubic to a distorted bct tetragonal structure: a slightly distorted $c/a > 1.05$ bct structure can rise the anisotropy of these alloys to the order of MJ/m^3 [34,35]. Despite the presence of preferred orientations for the Co NPs, the resolution of our structural XRD measurements do not allow to account for such a small degree of distortion. Certainly, further work at the nanoscale is being now performed in order to unravel the origin of such big magnetic anisotropy value.

4. Magnetorheological application

By following the same chemical reduction process previously described, we proceed to synthesize nearly equiatomic $Fe_{47}Co_{53}$ alloy composition, achieving as final product a good quality powder of the 30–50 nm size, with α-bcc body-centred FeCo structure, and maximum magnetization value of 212 Am^2/kg, remanence magnetization of 18 Am^2/kg and low hysteresis with coercivity field value about 7.1 kA/m. This alloy was used to fabricate a magnetorheological fluid (MRF) by using mineral oil as carrier liquid and Aerosil 300 as additive to control the viscosity of the fluid. The obtained fluid magnetorheological behavior was tested by using an Anton Paar Physica MCR 501 rotational rheometer provided with a MRD70/1T magnetorheological cell and parallel disk configuration (PP20/MRD/TI). Extensive information about this MRF fabrication and characterization can be found in [6].

Our measurements show non-Newtonian behaviour and strong magnetorheological response reflected in the increase of measured shear stress values as the applied magnetic field increases, being this change evident even for the smallest applied ones (see Fig. 5).

The post-yield (high shear rates) behavior of our $Fe_{47}Co_{53}$-MR fluid could be modelled by using the Herschel-Bulkley model [36] that consists in a parametric description of the form: $\tau = \tau_0 + K \bullet \dot{\gamma}^n$ where τ is the shear stress, τ_0 is the yield stress, $\dot{\gamma}$ is the shear rate, K is the consistency index (that gives an idea about the viscosity of the fluid) and n is the

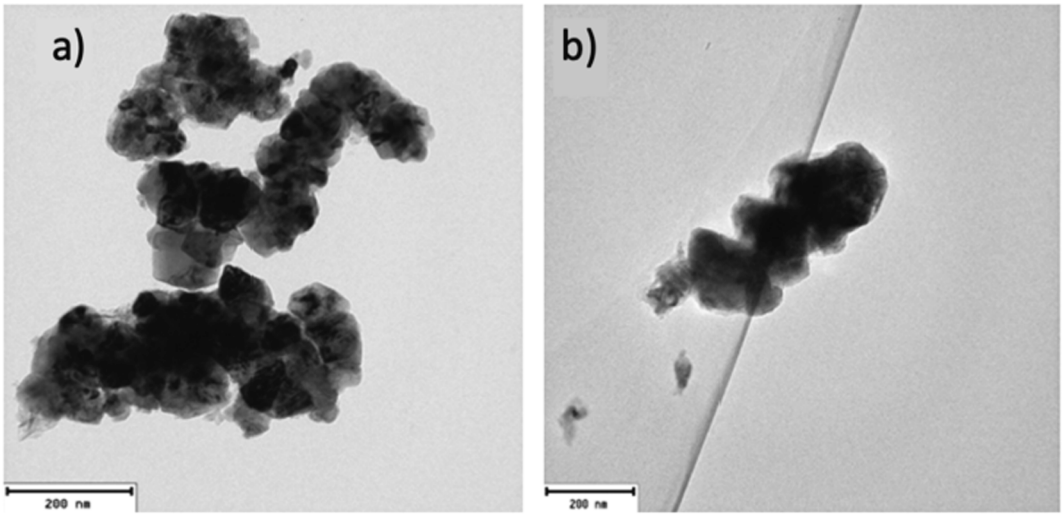

Fig. 2. TEM images of a) $Fe_{66}Co_{34}$ and b) $Fe_{33}Co_{67}$ compositions synthesized NPs.

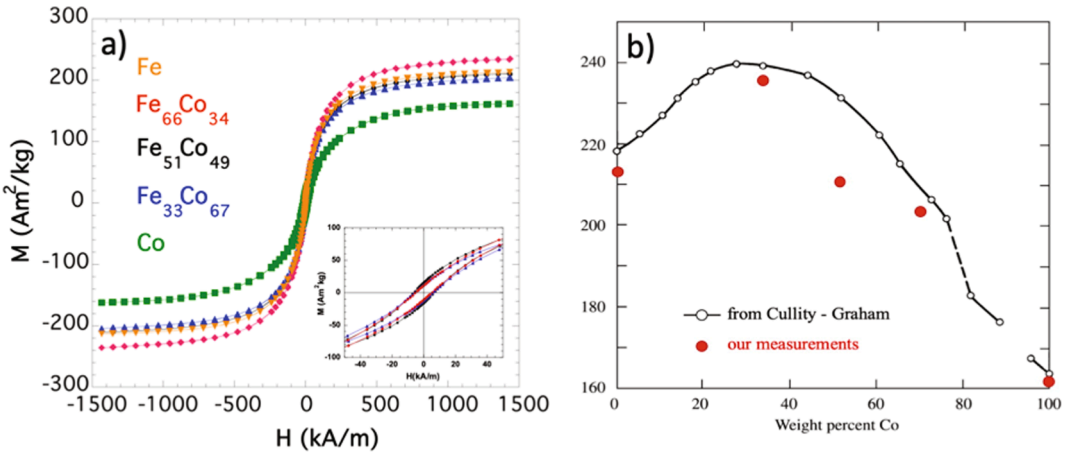

Fig. 3. a) Room temperature hysteresis loop of the Fe, Co and Fe_xCo_{1-x} NPs synthesized by the chemical reduction method. Inset shows an amplified zone of the Fe_xCo_{1-x} NPs hysteresis loop in order to observe the coercive field and the remanence; b) comparison between our measured saturation magnetization values and those reported in [25].

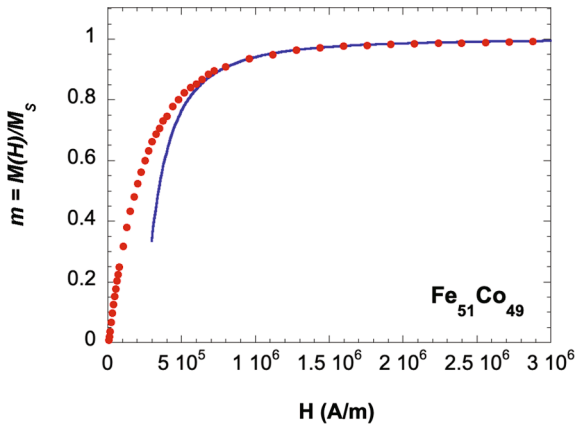

Fig. 4. Fit (blue solid line) to *law of approach to saturation* (LAS) for the synthesized $Fe_{51}Co_{49}$ alloy. Experimentally measured points are also shown as full red dots.

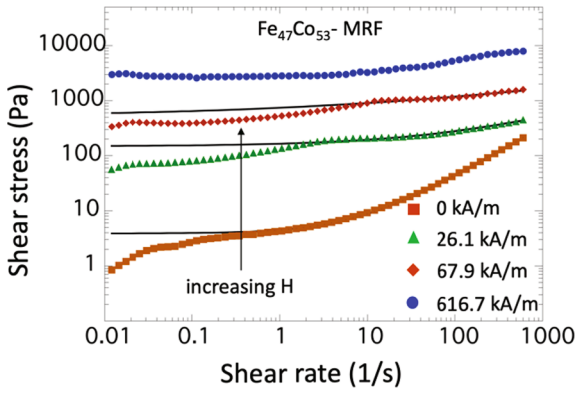

Fig. 5. Measured rheological curves as a function of the applied magnetic field for the new $Fe_{47}Co_{53}$-MR fluid showed in this work. Black lines show the Herschel-Bulkley fit, being this under blue dot symbols for the maximum applied field of 616.7 kA/m. Adapted from [6] with permission of the authors.

pseudo-plasticity or flow behaviour index (for pseudo-plastic fluids, $n < 1$) [36]. Fig. 5 shows the most representative measured curves, together with the corresponding Herschel-Bulkley fits. It is remarkable that for the maximum applied magnetic field, the fit line lies under the true measured experimental curve. In this case, values of $\tau_0 = 2729$ Pa, n = 0.5 and $K = 300$ Pa.s$^{0.5}$ have been determined. In particular, the yield stress value of$\tau_0 = 2729$ Pa competes well with the most recent results in the literature (see Table 2 in ref. [6]).

To test the reversibility of the previously observed behaviour, rheological curves after applying a magnetic field to the $Fe_{47}Co_{53}$-MR fluid and a subsequent demagnetization process have been also measured (see Fig. 6).

Our measurements show just a small decrease of an 9.8% (at a shear rate of 92 s^{-1}) in the measured shear stress value when we applied the maximum magnetic field (616.7 kA/m), respect to the zero applied field case. This is a strong improvement if compared to reversibility in the rheology of a magnetorheological fluid fabricated by using exactly the same methodology but with good quality Fe nanoparticles as magnetic fillers, that showed a reversibility decrease as high as a 31% [6].

5. Conclusions

By following the chemical reduction of metal precursors proces we have synthesized three FeCo alloys of composition $Fe_{66}Co_{34}$, $Fe_{51}Co_{49}$ and $Fe_{33}Co_{67}$ as well as pure Fe and Co, all of them as nanoparticles in the range 25–50 nm that easily aggregate to sizes of several hundreds of nanometers. Except pure Co that shows the expected hexagonal hcp structure, pure Fe and the FeCo alloys crystallize in the bcc cubic structure. Those last show excellent soft magnetic properties with low coercive fields (about 5–6 kA/m) and magnetic saturation values that reach 235 Am^2/kg for the $Fe_{66}Co_{34}$ alloy composition. Despite this soft magnetic character, the estimated magnetic anisotropy value by using the law of approach to saturation (LAS) method is about 2 MJ/m^3, being this observation still under study.

The performance of such FeCo nanoparticles when used in magnetorheological fluids has been tested with the $Fe_{47}Co_{53}$ composition, fabricated by the same chemical reduction procedure, as magnetic filler in a mineral oil-based fluid. The excellent reversible behaviour of the

Table 3
Saturation magnetization (M_s) coercive field (H_c) and remanence magnetization (M_r) of the different Fe, Fe_xCo_{1-x} alloys and Co NPs synthesized in this work.

Sample	M_s (Am^2/kg)	H_c (kA/m)	M_r (Am^2/kg)
Fe	213 (±4)	3,1 (±0.2)	8 (±1)
$Fe_{66}Co_{34}$	235 (±4)	5,1 (±0.2)	11 (±1)
$Fe_{51}Co_{49}$	211 (±4)	6,4 (±0.2)	16 (±1)
$Fe_{33}Co_{67}$	204 (±4)	5,8 (±0.2)	12 (±1)
Co	162 (±4)	17 (±0.2)	19 (±1)

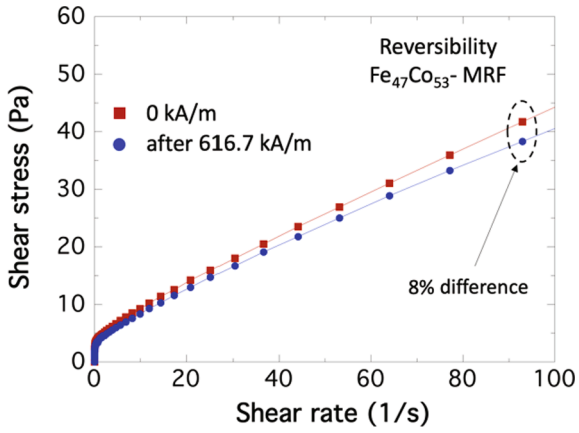

Fig. 6. Rheological curves after applying magnetic field and demagnetizing process for the new $Fe_{47}Co_{53}$-MR fluid. Adapted from [6] with permission of the authors.

fabricated fluid as well as the good determined yield stress value of 2729 Pa at high applied magnetic field fully support the use of high magnetization FeCo nanoparticles in MR fluids.

CRediT authorship contribution statement

Virginia Vadillo: Data curation, Investigation, Validation. **Maite Insausti:** Supervision, Methodology, Validation. **Jon Gutiérrez:** Supervision, Conceptualization, Methodology, Validation.

Declaration of Competing Interest

The authors declare that they have no known competing financial interests or personal relationships that could have appeared to influence the work reported in this paper.

Data availability

Data will be made available on request.

Acknowledgements

The authors would like to thank the financial support provided also by the Basque Government under MMMfavIN (KK-2020/00099), IDEA-II (KK-2021/00040) Elkartek Program and Research Groups (IT11479-22 and IT1546-22) projects. Technical and human support provided by the General Research Services of the UPV/EHU (SGIker) is gratefully acknowledged. In particular, extensive and deep discussions with Dr Iñaki Orue about magnetic behaviour of nanoparticles is truly appreciated.

Appendix A. Supplementary material

Supplementary data to this article can be found online at https://doi.org/10.1016/j.jmmm.2022.169975.

References

[1] T. Sourmail, Near equiatomic FeCo alloys: constitution, mechanical and magnetic properties, Prog. Mater Sci. 50 (2005) 816–880.
[2] J.M. MacLaren, T.C. Schulthess, W.H. Butler, R. Sutton, M. McHenry, Electronic structure, exchange interactions and Curie temperature of FeCo, J. Appl. Phys 85 (8) (1999) 4833–4835.
[3] N.O. Nuñez, M. Pedro Tartaj, P. Morales, P. Bonville, C.J. Serna, Y.-C. Nanoneedles, Chem. Mater. 16 (2004) 3119–3124.
[4] S. An, X. Li, W. Li, F. Ren, X.u. Panpan, Coercivity enhancement of SmCo/FeCo nanocomposite magnets by doping eutectic Sm-Zn alloy, Mater. Lett. 284 (2021), 128965.
[5] Ö. Çelik, T. Firat, Synthesis of FeCo magnetic nanoalloys and investigation of heating properties for magnetic fluid hyperthermia, J. Magn. Magn. Mat. 456 (2018) 11–16.
[6] V. Vadillo, A. Gómez, J. Berasategi, J. Gutiérrez, M. Insausti, I. Gil de Muro, J. S. Garitaonandia, A. Arbe, A. Iturrospe, M.M. Bou-Ali, J.M. Barandiarán, High magnetization FeCo nanoparticles for magnetorheological fluids with enhanced response, Soft Matter 17 (2021) 840–852, https://doi.org/10.1039/d0sm01702g.
[7] V. Tzitzios, G. Basina, D. Niarchos, W. Li, G. Hadjipanayis, Synthesis of air stable FeCo nanoparticles, J. Appl. Phys. 109 (2011) 07A313.
[8] B. Kandapallil, R.E. Colborn, P.J. Bonitatibus, F. Johnson, Synthesis of high magnetization Fe and FeCo nanoparticles by high temperature chemical reduction, J. Magn. Magn. Mater. 378 (2015) 535–538.
[9] G.S. Chaubey, C. Barcena, l.N. Poudya, C. Rong, J. Gao, S. Sun, J.P. Liu, Synthesis and stabilization of FeCo nanoparticles, J. Am. Chem. Soc. 129 (2007) 7214.
[10] N. Poudyal, G.S. Chaubey, C.-B. Rong, J. Cui, J. Ping Liu, Synthesis of monodisperse FeCo nanoparticles by reductive salt-matrix annealing, Nanotechnology 24 (2013) 345605 (6pp).
[11] Z.J. Huba, K.J. Carroll, E.E. Carpenter, Synthesis of high magnetization FeCo alloys prepared by a modified polyol process, J. Appl. Phys. 109 (2011) 07B514.
[12] M. Zamanpour, Y. Chen, B. Hu, K. Carroll, Z.J. Huba, E.E. Carpenter, L.H. Lewis, V. G. Harris, Large-scale synthesis of high moment FeCo nanoparticles using modified polyol synthesis, J. Appl. Phys. 111 (2012) 07B528.
[13] J. Peng, Z. Peng, L. Wang, L. Zheng, Z. Zhu, G. Li, T. Jiang, Microwave-assisted one-step synthesis of FeCo/graphene nanocomposite for microwave absorption in characterization of minerals, Met. Mater. (2015) 329–340.
[14] P. Narayah, C.-B. Rong, J.P. Liu, Morphological and magnetic characterization of Fe, Co and FeCo nanoplates and nanoparticles prepared by surfactants-assisted ball milling, J. Appl. Phys. 109 (2011) 07B526 (3 pp.).
[15] R. Gupta, K. Lieb, G. Muller, M. Wetssheit y K. Zang, Influence of substrate and ion irradiation on the magnetic properties of Laser-Deposited CoFe films, Nucl. Instrum. Methods. Phys. Res. Sec. B 246 (2006) 373–396.
[16] V. Vadillo, J. Gutiérrez, M. Insausti, J.S. Garitaonaindia, I. Gil de Muro, I. Quintana, J.M. Barandiarán, Synthesis and characterization of Fe-Co-V high-magnetization nanoparticles obtained by physical routes, IEEE Magnetic Lett. 10 (2019) 6104805 (5 pp.), doi: 10.1109/LMAG.2019.2934076.
[17] Z. Klencsár, P. Németh, Z. Sándor, T. Horváth, I.E. Sajo, S. Mészáros, J. Mantilla, J. A.H. Coaquira, V.K. Garg, E. Kuzmann, Gy Tolnai, Structure and magnetism of Fe-Co alloy nanoparticles, J. Alloys Compd. 674 (2016) 153–1116.
[18] T.P. Braga, D.F. Dias, M.F. de Sousa, J.M. Soares, J.M. Sasaki, Synthesis of air stable FeCo alloy nanocrystallite by proteic sol-gel method using a rotary oven, J. Alloys Compounds 622 (2015) 408–417.
[19] D. Kodama, K. Shinoda, K. Sato, Y. Konno, R.J. Joseyphus, K. Motomiya, H. Takahashi, T. Matsumoto, Y. Sato, K. Tohji, B. Jeyadevan, Chemical synthesis of sub-micrometer- to nanometer-sized magnetic FeCo dice, Adv. Mater. 18 (2006) 3154–3159.
[20] F.J. Yang, J. Yao, J.J. Min, J.H. Li, X.Q. Chen, Synthesis of high saturation magnetization FeCo nanoparticles by polyol reduction method, Chem. Phys. Lett. 648 (2016) 143–146.
[21] F. Sánchez-De Jesús, A.M. Bolarín-Miró, C.A. Cortés Escobedo, G. Torres-Villaseñor, P. Vera-Serna, Structural analysis and magnetic properties of FeCo alloys obtained by mechanical alloying, Hindawi Publishing Corporation, J. Metallurgy (2016) Article ID 8347063 (8 pages), doi: 10.1155/2016/8347063.
[22] Y. Wang, Y. Zheng, S. Hu, Synthesis of mono-dispersed Fe-Co nanoparticles with precise composition control, J. Phys. Chem. Solids 100 (2017) 78–82.
[23] C.A. Schneider, W.S. Rasband, K.W. Eliceiri, NIH image to ImageJ: 25 years of image analysis, Nat. Methods 9 (2012) 671–675.
[24] R. Harpeness, A. Gedanken, The microwave-assisted polyol synthesis of nanosized hard magnetic material FePt, J. Mat. Chem. 15 (2005) 698–702.
[25] B.D. Cullity, C.D. Graham, Introduction to Magnetic Materials, IEEE Press & John Wiley & Sons Inc. Publication, 2009, p. 142.
[26] J. Berasategi, A. Gomez, M.M. Bou-Ali, J. Gutiérrez, J.M. Barandiarán, I.V. Beketov, A.P. Safronov, G.V. Kurlyandskaya, Fe nanoparticles produced by electric explosion of wire for new generation of magneto-rheological fluids. Smart Mater. Struct. 27 (2018) 045011(8 pp.), doi: 10.1088/1361-665X/aaaded.
[27] S. Chikazumi, Physics of Ferromagnetism, second ed., Oxford University Press, New York, 1997.
[28] C. Caizer, Handbook of Nanoparticles, Chapter 9: Nanoparticle Size Effect on Some Magnetic Properties, in: M. Aliofkhazraei (Ed.), Springer International Publishing Switzerland, 2016.
[29] E. Becker, H. Polley, Ann. Phys. 37 (1940) 534.
[30] J.M.D. Coey, Magnetism and Magnetic Materials, Cambridge University Press, 2010.
[31] K. Zehani, R. Bez, A. Boutahar, E.K. Hlil, H. Lassri, J. Moscovici, N. Mliki, L. Bessais, Structural, magnetic, and electronic properties of high moment FeCo nanoparticles, J. Alloys Compd. 591 (2014) 58–64.
[32] E.M.M. Ibrahim, S. Hampel, A.U.B. Wolter, M. Kath, A.A. El-Gendy, R. Klingeler, ChristineTaschner, VyacheslavO.Khavrus, ThomasGemming, AlbrechtLeonhardt, B. Büchner, Superparamagnetic FeCo and FeNi nanocomposites dispersed in submicrometer-sized C spheres, J. Phys. Chem. C 116 (2012) 22509−22517.
[33] I. Arief, S. Biswas, S. Bose, Tuning the shape anisotropy and electromagnetic screening ability of ultrahigh magnetic polymer and surfactant-capped FeCo nanorods and nanocubes in soft conducting composites, ACS Appl. Mater. Interfaces 8 (2016) 26285–26297.
[34] J. Bansmann, A. Kleibert, M. Getzlaff, A.F. Rodriguez, F. Nolting, C. Boeglin, K.-H. Meiwes-Broer, Magnetism of 3d transition metal nanoparticles on surfaces probed

with synchrotron radiation – from ensembles towards individual objects, Phys. Status Solidi B 247 (5) (2010).
[35] T. Hasegawa, T. Niibori, Y. Takemasa, M. Oikawa, Stabilisation of tetragonal FeCo structure with high magnetic anisotropy by the addition of V and N elements, Sci. Rep. 9 (2019), 5248 (9 pp).
[36] T.G. Mezger, The rheology handbook, Vincentz Network, Germany, 2002.